Molecular Pharmacology Fast Forward. Published on October 22, 2018 as DOI: 10.1124/mol.118.113183
This article has not been copyedited and formatted. The final version may differ from this version.

MOL #113183

Substrate-Induced Motion between TM4 and TM7 of the Glutamate Transporter EAAT1 Revealed by Paired Cysteine Mutagenesis

Wenlong Zhang, Xiuping Zhang and Shaogang Qu

Primary Laboratory of Origin:

Central Laboratory, Shunde Hospital, Southern Medical University (The First People's Hospital of Shunde Foshan), Foshan, Guangdong, China (WLZ, SGQ)

Key Laboratory of Mental Health of the Ministry of Education, Southern Medical University, Guangzhou, Guangdong, China (WLZ, SGQ)

Teaching Center of Experimental Medicine, School of Basic Medical Sciences, Southern Medical University, Guangzhou, Guangdong, China (XPZ)

Downloaded from molpharm.aspetjournals.org at ASPET Journals on April 17, 2024

Molecular Pharmacology Fast Forward. Published on October 22, 2018 as DOI: 10.1124/mol.118.113183
This article has not been copyedited and formatted. The final version may differ from this version.

MOL #113183

Running Title:

Substrate-Induced Motion between TM4 and TM7 of EAAT1

Corresponding Author:

Shaogang Qu, Central Laboratory, Shunde Hospital, Southern Medical University, Foshan, Guangdong 528300, China

Voice:+86 757 22819316

Fax: +86 757 22223899

Email: sgq9528@163.com

Number of text pages: 18

Number of Tables: 0

Number of Figures: 7

Number of References: 46

Number of words in Abstract: 226

Number of words in Introduction: 648

Number of words in Discussion: 1491

Abbreviations: HP, hairpin loop; TM, transmembrane domain; DTT, DL-dithiothreitol; MTSET, (2-trimethylammonium) ethyl methanethiosulfonate; EAATs, excitatory amino acid transporters; Glt_{Ph}, glutamate transporter homologue from *Pyrococcus horikoshii*; CuPh, copper phenanthroline; MTSEA, 2-aminoethyl methanethiosulfonate; CL-EAAT1, Cysteine-less EAAT1; DL-TBOA, D, L-threo-β-benzyloxy-aspartate.

Downloaded from molpharm.aspetjournals.org at ASPET Journals on April 17, 2024

Molecular Pharmacology Fast Forward. Published on October 22, 2018 as DOI: 10.1124/mol.118.113183
This article has not been copyedited and formatted. The final version may differ from this version.

Abstract

In order to maintain efficient synaptic communication, glutamate transporters re-uptake glutamate from the synaptic cleft and prevent glutamate concentrations from reaching neurotoxic levels. The number of amino acid residues of TM (transmembrane domain, TM) 4b-4c loop of mammalian EAATs is 50 amino acids more than that of prokaryotic homologue. To investigate the spatial proximity and functional significance of residues in glutamate transporter, cysteine pairs were introduced at positions A243 of TM4b-4c loop and T396 or A414 of TM7, respectively. The transport activity of double mutants A243C/T396C and A243C/A414C was inhibited by Cu(II)(1,10-phenanthroline)$_3$ (CuPh) and cadmium ions, but the uptake activity of corresponding single mutants remained unchanged. Treatment with dithiothreitol after CuPh restored much of the transport activity. The inhibitory effects of CuPh and cadmium could only be detected when cysteine pairs are in the same polypeptide. Therefore, we suggest that the formation of these disulfide bonds occurs intra-molecularly. Glutamate, potassium and DL-TBOA facilitated cross-linking in the A243C/T396C transporter and this suggests that TM4b-4c loop and β-bridge region in TM7 were drawn into close proximity to each other in the inward-facing and outward-facing conformation of EAAT1. Thus, these data provide evidence that substrate-induced structural rearrangements occur between TM4b-4c loop and TM7 during the transport cycle.

Downloaded from molpharm.aspetjournals.org at ASPET Journals on April 17, 2024

Molecular Pharmacology Fast Forward. Published on October 22, 2018 as DOI: 10.1124/mol.118.113183
This article has not been copyedited and formatted. The final version may differ from this version.

Introduction

Glutamate is the primary excitatory neurotransmitter in the mammalian central nervous system. It is continually pumped into the cytoplasm to prevent hyperexcitability and neurotoxicity by excitatory amino acid transporters (EAATs) located in the plasma membranes of glial cells and neurons (Amara and Fontana, 2002; Kanai and Hediger, 2004). Five members of the glutamate transporter (EAAT1–EAAT5 transporters), expressed at the plasma membrane of glial cells and neurons, have been cloned (Arriza et al., 1997; Arriza et al., 1994; Fairman et al., 1995; Kanai and Hediger, 1992; Pines et al., 1992; Storck et al., 1992). They showed an overall amino acid identity of ~50% (Arriza et al., 1997). EAAT1 and EAAT2 are responsible for most of the glutamate uptake in the rodent brain (Lehre and Danbolt, 1998). Glutamate uptake is an electrogenic process facilitated by Na^+-K^+-ATPase (Brew and Attwell, 1987; Kanner and Sharon, 1978; Wadiche et al., 1995), where the transport cycle causes the binding of substrate together with three sodium ions and one proton. Upon binding, these are released into the cytoplasm and the transporter for the next cycle is reset following the counter transport of a single potassium ion (Levy et al., 1998; Pines et al., 1995; Zerangue and Kavanaugh, 1996). Crystal structures from *Pyrococcus horikoshii* (Glt_{Ph}) have advanced our insight about the glutamate transporter (Boudker et al., 2007; Reyes et al., 2009; Verdon and Boudker, 2012; Yernool et al., 2004). Glt_{Ph} is a trimer where each monomer is a functional unit (Yernool et al., 2004). The protomer contains eight transmembrane domains (TM1–TM8) and two oppositely oriented hairpin loops, one between domains 6 and 7 (HP1) and the other between domains 7 and 8 (HP2). HP2 has been suggested to act as the extracellular gate to bind the substrate, while HP1 has been demonstrated to act as the intracellular gate. (Boudker et al., 2007; Canul-Tec et al., 2017; Crisman et al., 2009; Qu and Kanner, 2008; Shrivastava et al., 2008; Teichman et al., 2009; Yernool et al., 2004). It's a common phenomenon for the eukaryotic glutamate transporters and thus it serves as a model which can be used to probe conformational changes driving transport in the EAATs (Grewer et al., 2005; Koch et al., 2007a; Koch and Larsson, 2005; Leary et al., 2007). In addition, the unusual topology of Glt_{Ph} is highly consistent with that of eukaryotic transporters which has been studied in biochemistry. (Boudker et al., 2007; Crisman et al., 2009; Teichman et al., 2009). However, Glt_{Ph} only shares ~35% sequence identity with the EAATs (Slotboom et al., 1999; Yernool et al., 2004). The amino acid insertions or deletions may make this homologue a limited structural model to uncover the molecular mechanism of the EAATs proteins. There are more 53 amino acid residues in the TM4b-4c loop of EAAT1 than Glt_{Ph} (Yernool et al., 2004) (Fig. 1A). Additionally, it had been declared that the transport domain, which included TM3, TM6–TM8 and re-entrant helical loops (HP1 and HP2), moved relatively to the scaffold domain, including transmembrane helices TM1–

Downloaded from molpharm.aspetjournals.org at ASPET Journals on April 17, 2024

Molecular Pharmacology Fast Forward. Published on October 22, 2018 as DOI: 10.1124/mol.118.113183
This article has not been copyedited and formatted. The final version may differ from this version.

TM2 and TM4–TM5(Crisman et al., 2009; Groeneveld and Slotboom, 2007; Reyes et al., 2009).

In order to investigate the spatial location change between TM4b-4c loop and TM7 during the transport cycle, we performed the study of oxidative cross-linking. (Fig. 1A, B, C). We designed double cysteine transporters by introducing pairs of cysteine residues on cysteine-less version of EAAT1, substitutions for the three endogenous cysteine residues, C186S, C252A, and C375G, leading to about 75% transport activity of the wild-type EAAT1 (Seal and Amara, 1998). Transport activity of double cysteine transporters was detected in the presence or the absence of CuPh, a catalyzer of disulfide bond formation. We also examined the effects of substrates, inhibitors, and potassium ions on the inhibition of crosslinking, and the effect of external media on the inhibition of transport activity by sulfhydryl modification in a single cysteine mutant. Our results indicated that the complex spatial relationship and proximity between TM7 and TM4b-4c loop are altered during the transport cycle.

Materials and methods

Generation and subcloning of mutants

The cysteine-less EAAT1 (*Rattus norvegicus*, GenBank: X63744.1) is constructed in the vector pBluescript SK(-)(Stratagene, La Jolla, CA, USA). Cysteine-less EAAT1 serves as a template for site-directed mutagenesis. QuikChange Site-Directed Mutagenesis Kit (TOYOBO, Osaka, Japan) and PCR was used to generate mutant transporters. All mutant transporters were ascertained by full-length sequencing (Sangon Biotech, Shanghai, China).

Cell Culture and Transient Transfections

HeLa cells were purchased from ATCC and grown on a 24-well plate using Dulbecco's Modified Eagle's Medium (Thermo Fisher Scientific, Waltham, MA, USA)containing 10% fetal calf serum (ExCell Biology, Shanghai, China), 200 U/ml penicillin, and 200 μg/ml streptomycin (Beyotime Biotechnology, Shanghai, China). After 20 h, HeLa cells were transiently infected with recombinant vaccinia/T7 virus vTF (Fuerst et al., 1986). The CL-EAAT1 or mutant constructs were transfected into HeLa cells with Lipo6000™ Transfection Reagent (Beyotime Biotechnology, Shanghai, China) and cultured at 37 ℃, 5% CO_2 for 20 h.

Transport assay

HeLa cells expressing the mutant were washed once with 1 mL choline chloride (ChCl) solution (150 mM ChCl, 5 mM KPi, pH 7.4, 0.5 mM $MgSO_4$, and 0.3 mM $CaCl_2$) after transfection for 20 h. Then, the NaCl solution [150 mM NaCl, 5 mM KPi, pH 7.4, 0.5 mM

Downloaded from molpharm.aspetjournals.org at ASPET Journals on April 17, 2024

Molecular Pharmacology Fast Forward. Published on October 22, 2018 as DOI: 10.1124/mol.118.113183
This article has not been copyedited and formatted. The final version may differ from this version.

$MgSO_4$, and 0.3 mM $CaCl_2$] containing 0.4 μCi (0.15 μM) D-[^{3}H]-aspartate (PerkinElmer, MA, USA) was added to incubate cells for 10 min. Ice cold NaCl solution was added to terminate the reaction, followed by washing twice with NaCl solution. 1% SDS was added to lyse cells and radioactivity was detected. All data were calculated after subtracting the value of the transfection of vector pBluescript SK (-).

Cell surface Biotinylation

Cell surface expression levels of mutants were examined using the membrane-impermeable biotinylation reagent EZ-Link™ Sulfo-NHS-SS-biotin (Thermo Scientific, Waltham, MA, USA). HeLa cells transfected with CL-EAAT1 or mutants were washed twice with ice-cold PBS (PH 8.0), and then incubated with EZ-Link™ Sulfo-NHS-SS-biotin (0.5 mg/ml in PBS) for 20 min. Cells were washed twice with 100 mM glycine to terminate the reaction. Then, the cells were lysed on ice with cell lysis buffer [20 mM Tris (pH7.4), 150 mM NaCl, 1% Triton X-100, sodium pyrophosphate, β-glycerophosphate, EDTA, Na_3VO_4, leupeptin, and 1mM PMSF] for 20 min, and the supernatants (i.e., the total proteins) were collected after centrifugation (12,000 rpm for 20 min at 4℃). The cell debris was discarded. Pierce™ Streptavidin Agarose (Thermo Scientific, Waltham, MA, USA) was added to bind the biotin-labeled cell membrane proteins for 1 h at 4℃. Streptavidin-agarose beads were centrifuged 12000 rpm for 1 min at 4℃. Supernatants (the non-biotinylated proteins) were removed to new tubes. Streptavidin-agarose beads were washed three times through 1 mL ice cold lysis buffer to remove the non-biotinylated proteins. Centrifugation was performed at 12000 rpm for 1 min at 4℃. The membrane protein samples (the biotinylated proteins), total proteins and non-biotinylated proteins were used for western blot (Rong et al., 2016).

Western blot analysis

Samples were mixed with protein loading buffer and boiled at 55℃ for 30 min. Protein samples were fractionated by 10% SDS-PAGE and transferred onto polyvinylidene difluoride membranes. Blocked with 5% BSA for 1.5 h at room temperature. The membranes were incubated with anti-EAAT1 antibody (Santa Cruz, CA, USA) for 16 h at 4℃. Integrin (Santa Cruz, CA, USA), α/β-tubulin (Santa Cruz, CA, USA) and β-actin (Beyotime Biotechnology, Shanghai, China) were used as internal controls. Then, the blots were incubated with secondary antibodies for 1 h at room temperature. Secondary antibodies were HRP-labeled Donkey Anti-Goat IgG (H+L) for EAAT1 and Integrin, HRP-labeled Goat Anti-Mouse IgG(H+L) for β-actin, and HRP-labeled Goat Anti-Rabbit IgG(H+L) for α/β-tubulin. All secondary antibodies were purchased from Beyotime Biotechnology (Shanghai, China). The

Downloaded from molpharm.aspetjournals.org at ASPET Journals on April 17, 2024

Molecular Pharmacology Fast Forward. Published on October 22, 2018 as DOI: 10.1124/mol.118.113183
This article has not been copyedited and formatted. The final version may differ from this version.

blots were detected by chemiluminescent BeyoECL Plus (Beyotime Biotechnology, Shanghai, China) Membrane polymer protein expression, the non-biotinylated proteins and the total proteins were calculated by the optical density of bands for CL-EAAT1 and its mutants divided by the corresponding value for integrin, α/β-tubulin and β-actin expression in individual samples. Membrane expression, the non-biotinylated proteins, and the total proteins of CL-EAAT1 were designated as 100%. The uptake activity of mutant was normalized to the expression of membrane protein as the relative intrinsic activity, which was calculated as follows: the uptake activity of mutant/the expression of membrane protein polymer in mutant.

Inhibition of transport by CuPh

After HeLa cells transfected with CL-EAAT1 and mutant for 18–20 h in 24-well plates, ChCl solution was added to wash the cells twice, and then the cells were incubated with different concentrations of CuPh at room temperature for 5 min, followed by washing twice with ChCl solution. Uptake activity was detected as described above. CuPh stock solution was prepared by mixing 400 μl of 1.25 M 1,10-phenanthroline in water: ethanol (1:1) and 600 μl of 250 mM $CuSO_4$. The aim of the concentration curve was to explore a concentration where CuPh caused a partial inhibition and the effects of the different external media could be showed most clearly.

Restoration of activity with dithiothreitol

HeLa cells expressing CL-EAAT1 and mutants were washed twice with ChCl solution. The corresponding concentration of CuPh was added and incubated at room temperature for 5 min. The incubated solution was discarded and the cells washed twice with ChCl solution. Next, NaCl solution containing 20 mM DTT was added and the cells incubated for 5 min. The incubated solution was discarded, the cells were washed twice with ChCl solution, and the transport activity of the mutant was detected.

Inhibition of transport by Cd^{2+}

HeLa cells expressing CL-EAAT1 and mutants were washed twice with ChCl solution. 500 mM cadmium chloride in transport solution [150 mM NaCl, 5 m MKPi (pH7.4), 0.5 mM $MgSO_4$, and 0.3 mM $CaCl_2$] was added and incubated at room temperature for 5 min. The incubated solution was discarded, the cells washed twice with ChCl solution, and the transport activity of mutant detected.

Downloaded from molpharm.aspetjournals.org at ASPET Journals on April 17, 2024

Molecular Pharmacology Fast Forward. Published on October 22, 2018 as DOI: 10.1124/mol.118.113183
This article has not been copyedited and formatted. The final version may differ from this version.

Effects of external media on oxidative inhibition by CuPh or sulfhydryl reagent

HeLa cells expressed CL-EAAT1 and mutants were washed with 1 mL ChCl solution. Cells were incubated with different external media contained with or without the indicated concentrations of CuPh or sulfhydryl reagent for 5 min at room temperature. The media contained one of the following: NaCl solution, NaCl solution + 1 mM L-glutamate, NaCl solution + 20 μM D, L-threo-β-benzyloxyaspartate (DL-TBOA) (Tocris, Bristol, UK), KCl solution [150 mM KCl, 5 mM KPi, pH 7.4, 0.5 mM $MgSO_4$, and 0.3 mM $CaCl_2$], or ChCl solution. The medium was sequentially removed and cells were washed twice with the ChCl solution. Transporter-mediated D-[^{3}H]-aspartate uptake was detected. Each experiment was performed at least three times.

Statistical analysis

Data are presented as the mean ± SD from three independent experiments. Data analysis was performed with SPSS 20.0 statistical software using one-way ANOVA with post-hoc comparison via the Dunnet test. Data were considered statistically significant at $P < 0.05$ or $P < 0.01$.

Results

Effects of Cysteine Cross-linking on Transport activity

We constructed 26 double cysteine transporters between A243C on TM4b-4c loop and TM7 for this cross-linking study. We identified two double cysteine transporters, A243C/T396C and A243C/A414C (Fig. 2A) exhibiting a decrease in transport activity after exposure to CuPh. The other transporter mutants showed no change in transport activity after exposure to CuPh. The activity of the A243C/T396C and A243C/A414C was inhibited by CuPh in a dose-dependent manner (Fig. 2B, C). Preincubation of HeLa cells expressing the double mutant with 600 μM CuPh resulted in inhibition of transport by more than 35% (Fig. 2B, C). Very little inhibition was seen with single mutant, similar to results with CL-EAAT1 (Fig. 2D). Except for A243C, all other mutants exhibited lower transport activity than CL-EAAT1 (Fig. 2E).

Expression of cysteine mutants

To determine the association between decreased transport activity and membrane expression of the mutant, surface biotinylation was performed. Cell surface expression of mutants was measured using membrane-impermeable biotin labeling and immunoblotting supplemented with densitometric analysis of developed bands (Fig. 3A). The total protein content of A243C/T396C and A243C/A414C show a slight decrease than CL-EAAT1 (Fig.

Downloaded from molpharm.aspetjournals.org at ASPET Journals on April 17, 2024

Molecular Pharmacology Fast Forward. Published on October 22, 2018 as DOI: 10.1124/mol.118.113183
This article has not been copyedited and formatted. The final version may differ from this version.

3B). Cell surface expression of A243C/T396C and A243C/A414C exhibited a pronounced decline as shown in Fig. 3 (A, C). The expression of non-biotinylated proteins of A243C/T396C and A243C/A414C declined compared to CL-EAAT1 (Fig. 3A, D). Compared with CL-EAAT1, uptake activity normalized to relative cell surface expression of all mutants decreased (Fig. 3E). Although, the ratio of biotinylated proteins to non-biotinylated proteins showed no statistically significant decrease (Fig. 3F).

Effects of dithiothreitol on cross-linking in double cysteine transporters

To determine whether the effect of CuPh treatment on the two double cysteine transporters was reversible, HeLa cells expressing A243C/T396C and A243C/A414C were first incubated with CuPh and then with the reducing agent, DL-dithiothreitol (DTT). DTT restored transport activity of both paired cysteine transporters. While the transport activities of A243C/T396C and A243C/A414C were inhibited to 45.5 ± 5.1% and 60.6 ± 4.1% by the application with 600 μM CuPh, 20 mM DTT restored the transport activities of the double mutants up to 90.7 ± 8.9% and 95.5 ± 7.6% (Fig. 4A, B). We also confirmed that DTT had no effect on the activity of CL-EAAT1 (data not shown).

Inhibition of transport of cysteine mutants by Cadmium.

To determine whether the amino acid sites A243C and T396C or A243C and A414C in the mutant were close in space, we assessed the effects of cadmium. Cadmium, the divalent cation, is known to interact with cysteinyl side chains and it has been shown that the affinity of interaction is increased dramatically if Cd^{2+} ion can be coordinated by two cysteines (Glusker, 1991; Perez-Garcia et al., 1996). Exposure of the single mutant (A243C, T396C, A414C or CL-EAAT1) to 500 μM Cd^{2+} had very little effect on D-[^{3}H]-aspartate uptake (Fig. 4C, D). Comparatively, inhibition was observed on uptake by double cysteine transporters A243C/T396C (31.9 ± 3.4% of control) and A243C/A414C (63.9 ±3.6% of control) mutant (Fig. 4C, D). These results support the intramolecular spatial proximity of A243C and T396C, or A243C and A414C.

Effect of external media on cross-linking in double cysteine transporters

To investigate the effect of substrate transport and inhibitor binding on disulfide cross-linking of cysteine pairs, Hela cells expressing A243C/T396C and A243C/A414C were incubated with CuPh supplemented external media. Glutamate and potassium increase the proportion of inward-facing conformation, while DL-TBOA increases the proportion of

Downloaded from molpharm.aspetjournals.org at ASPET Journals on April 17, 2024

Molecular Pharmacology Fast Forward. Published on October 22, 2018 as DOI: 10.1124/mol.118.113183
This article has not been copyedited and formatted. The final version may differ from this version.

transporters in the outward-facing conformation (Boudker et al., 2007; Reyes et al., 2009; Shlaifer and Kanner, 2007). Addition of glutamate, potassium or DL-TBOA augmented the disulfide bond formation in the A243C/T396C mutant (Fig. 5A). While addition of glutamate reduces disulfide bound formation in A243C/A414C, potassium and DL-TBOA showed no effect on A243C/A414C (Fig. 5B).

Aqueous accessibility of single cysteine transporters T396C and A414C

We used membrane-impermeable sulfhydryl reagent MTSET and membrane-permeable MTSEA for aqueous accessibility of individual cysteines. Sulfhydryl reagent can interact with cysteine residue and form a disulfide bond. This reaction can lead to variable degrees of loss of function of the glutamate transporter, depending on the location of the cysteine and the importance of that position to the function of the glutamate transporter. MTSET can interact with cysteine residue from the extracellular side. However, MTSEA can permeate the membrane and interact with cysteine residue from either side of the membrane (Holmgren et al., 1996). Cells expressing CL-EAAT1, T396C and A414C were pre-incubated in the presence of MTSET (Fig. 6A). A414C was found to be sensitive to MTSET (Fig. 6A) since its transport activity was inhibited by 0.5 mM MTSET. However, T396C was not impacted by MTSET (Fig. 6A). Different external media do not affect the inhibition of A414C by MTSET (Fig. 6B). To further investigate accessibility of single cysteine T396C and A414C from cytoplasm, cells expressing CL-EAAT1, T396C and A414C were pre-incubated in the presence of MTSEA (Fig. 6C). The activity of the T396C and A414C was inhibited by MTSEA in a dose-dependent manner and full inhibition of transport activity of T396C was observed with increased MTSEA concentration to 5.0 mM (Fig. 6C). Protection was observed in the presence of glutamate, potassium and DL-TBOA by MTSEA in T396C (Fig. 6D). No effect on inhibition of transport activity was observed by MTSEA in A414C in with different external media (Fig. 6E).

Discussion

Our previous results suggested that introduction of a pairwise cysteine substitutions between TM2 and TM4 domains caused the glutamate transporter EAAT2 to undergo a complex conformational shift during transport cycle (Rong et al., 2016). However, TM2 is the constituent of scaffold domain and has been considered to maintain the relative balance of the transporter during the translocation of substrate (Canul-Tec et al., 2017; Yernool et al., 2004). Thus, we assumed that the TM4 domains might participate in the translocation of substrate. Furthermore, N-glycosylation sites in the TM4 are also observed in human SLC1 transporters, which suggest that this loop may play a significant part in the post-translational processing of transporters (Canul-Tec et al., 2017). Some amino acid mutations and deletions were made in

Downloaded from molpharm.aspetjournals.org at ASPET Journals on April 17, 2024

Molecular Pharmacology Fast Forward. Published on October 22, 2018 as DOI: 10.1124/mol.118.113183
This article has not been copyedited and formatted. The final version may differ from this version.

the TM4b-c loop of the structure of EAAT1 cryst mutant, so most residues in the TM4b-4c loop could not been modeled (Canul-Tec et al., 2017). Previous studies have postulated that amino acid residues in TM4b-4c loop present in the mammalian EAATs were accessible to the extracellular region (Grunewald et al., 1998; Pines et al., 1992; Seal et al., 2000). Fluorescence resonance energy transfer analysis (FRET) also indicated that the TM4b-4c loop was accessible to the extracellular media (Koch and Larsson, 2005). TM7 is divided at the cell surface by β-bridge into two helices and constitutes one part of the translocation pore for substrates and co-transported ions (Seal and Amara, 1998). We have previously demonstrated that Ala243 on TM4 forms disulfide cross-linking to HP1 or HP2 (Rong et al., 2014). We also suggested that Ala243 on TM4b-4c loop was conformationally sensitive and might play a role in the transport pathway during the transport cycle (Zhang et al., 2018). To determine the spatial proximity and functional significance of residues in glutamate transporter, EAAT1, we created pairs of cysteine residues in A243 on TM4b-4c loop and β-bridge region of TM7 or the tip of TM7, and assessed the effect of disulfide cross-linking with CuPh on transport activity. We authenticated two double cysteine transporters, A243C/T396C and A243C/A414C, which exhibit decreased transport activity when exposed to CuPh (Fig. 2A, B, C, D). We observed that increasing concentrations of CuPh (1–600 μM) lead to a greater reduction in glutamate transport for both transporters (Fig. 2B, C). To determine whether there was a decrease in the expression of inactive mutant transporters at the plasma membrane or if the mutations intrinsically affected transport activity, surface biotinylation was performed. The decreased transport activity of A243C/T396C and A243C/A414C can in part be explained by the inability of the transporters to traffic into the plasma membrane, as evidenced by their dramatic absence from the biotinylated fraction (Fig. 3A, C). Uptake activity normalized to relative cell surface expression also shows that all mutants have an intrinsic transport defect (Fig. 3E).

CuPh can lead to the formation of covalent links between cysteines, and the reversibility in the presence of DTT confirms the formation of a disulfide bond. Transport activity was restored with 20 mM DTT in both double cysteine transporters (Fig. 4A, B). Additionally, transport activity in single mutants was unaffected by incubation with CuPh. Thus, we demonstrated that disulfide bonds formed in the A243C/T396C and A243C/A414C were reversible and occurred within single subunits rather than between multiple subunits. A complementary approach to assess the proximity between cysteines in TM4b-4c loop and TM7 is incubated with cadmium. The transport activity of double mutants was decreased and formed a high-affinity Cd^{2+} binding site (Fig. 4C, D). This result was in accordance to the inhibition of CuPh, which further suggested that A243 on TM4b-4c loop was in close proximity to T396 and A414 on TM7.

Downloaded from molpharm.aspetjournals.org at ASPET Journals on April 17, 2024

Molecular Pharmacology Fast Forward. Published on October 22, 2018 as DOI: 10.1124/mol.118.113183
This article has not been copyedited and formatted. The final version may differ from this version.

To maximize the effect of the change of disulfide cross-linking of cysteine pairs in the double cysteine mutants, cells expressing mutants were exposed to CuPh in the presence of different external media. DL-TBOA and the non-transported and competitive inhibitors are thought to bind similar sites as substrates, either inducing or stabilizing particular conformations. It was expected to increase the proportion of outward-facing transporters (Boudker et al., 2007). On the contrary, binding of L-glutamate might either directly block the access of other reagents to the cysteine side chain or stabilize a particular conformation such that access to the side chain is restricted. It is expected that the proportion of inward-facing transporters will be increased in the presence of glutamate (Reyes et al., 2009). It is also believed that the potassium relocation step is the rate-limiting step during the transport cycle and hence the proportion of inward-facing transporters is expected to increase when external potassium replaces sodium (Bergles et al., 2002). Transport activity was reduced when glutamate or potassium or DL-TBOA was co-incubated with CuPh in A243C/T396C (Fig. 5A). This indicated that disulfide bond formation increased and the transport activity was impaired. It can be observed that during transport cycle not only outward-facing but also inward-facing transporters cause A243C to come into close proximity to T396C of β-bridge region in TM7. The β-bridge region in TM7 might undergo significant inward motion relative to TM4 of the scaffold domain in the outward-facing and inward-facing transporters. In the case of the A243C/A414C transporter, transport activity was increased upon co-incubation of glutamate with CuPh (Fig. 5B). However, there may be uncertainties as the protective effect in the experiment is only about 10%, even though $p<0.05$. Furthermore, A414C, which is on the very tip of TM7, can cross-link with A243C, which is expected to be near the beginning of TM4c. This implies a very large incursion of the transport domain, much deeper than observed in crystal structures of Glt_{Ph}. Most of the glutamate transporters will form cross-links between TM4b-4c and TM7 on outward-facing or inward-facing transporters phases. This does not rule out the possibility that the TM4b-4c loop may be sufficiently flexible and that cross-links with TM7 are in rare interludes for a few transporters. Cα-Cα distances from the crystal of Glt_{Ph} between V151 and T308 or A326, which are equivalent to A243 and T396 or A414 of EAAT1, are similar in the substrate-binding and outward-facing, but not in the inward-facing, structures (8.7, 8.1, and 20.3 Å for V151 to T308; 35.7, 35, and 18.7 Å for V151 to A326) (Fig. 7). Our results are inconsistent with these data. The mechanism and structure of TM4b-4c loop in eukaryotic glutamate transporter may differ from that of Glt_{Ph} for the differences in quantity of residues. The extra 53 amino acid residues of TM4b-4c loop in EAAT1 may lead to the differences in spatial or configurational proximity during the transport cycle as compared to that of Glt_{Ph}.

Downloaded from molpharm.aspetjournals.org at ASPET Journals on April 17, 2024

Molecular Pharmacology Fast Forward. Published on October 22, 2018 as DOI: 10.1124/mol.118.113183
This article has not been copyedited and formatted. The final version may differ from this version.

The alteration of inhibitory effect of CuPh in double cysteine transporters may be explained as the change of proximity between TM4b-4c loop and TM7 or the modification of accessibility of the single cysteine residues. A414C was inhibited by MTSET, while T396C was not sensitive to MTSET (Fig. 6A). These results are consistent with previous data (Seal and Amara, 1998). T396C was sensitive to MTSEA, but glutamate, potassium, and DL-TBOA protected T396C against MTSEA.(Fig. 6C, D). There are two possibilities: the reduced accessibility of T396C in the inward- or outward-conformational states or the close proximity of T396 to the substrate or sodium binding sites. In the presence of sodium, when fully loaded with glutamate or TBOA, that position is likely to be protected from reacting with MTSEA (Boudker et al., 2007; Shrivastava et al., 2008). Our previous results demonstrated that A243C is accessible to MTSET and the inhibition was augmented in the presence of DL-TBOA (Rong et al., 2014). Upon investigation of the alteration of inhibitory effect of CuPh in different external media, we indicated that complex spatial relationship and proximity issues might occur between TM4 and TM7 during the transport cycle. State-dependent trypsin cleavage sites were found between TM3 and TM4 and conformational changes might occur during glutamate transport cycle in EAAT2 (Bergles et al., 2002; Grunewald and Kanner, 1995). To a certain extent, it was similar to our research data. However, very little conformational changes occur in TM4b-4c loop as assayed by fluorescence resonance energy analysis (FRET) (Koch and Larsson, 2005). FRET analysis cannot reflect true complex conformational changes because it just displays the mean of FRET efficiency. However, single-molecule fluorescence resonance energy transfer (smFRET) imaging observed large-scale transport domain movements in TM4 of Glt_{ph} (Akyuz et al., 2013). These data were consistent with our findings. It was also presumed that the TM4b-4c loop might take part in making extensive contacts within or between monomers (Koch et al., 2007b). Moreover, we have suggested that the glutamate transporter EAAT1 may undergo a complex spatial shift between TM4 and HP1 or HP2 during the transport cycle by paired cysteine mutagenesis (Rong et al., 2014). However, it has been shown that structural rearrangements were observed and TM7 can be cross-linked to TM8, HP1, or HP2 by chemical cross-linking of introduced cysteine pairs in EAAT1 (Leighton et al., 2006; Qu and Kanner, 2008). TMs 7 and 8 and the re-entrant loops form the binding pocket of Glt_{Ph} (Yernool et al., 2004). Together, these observations indicate that TM4b-4c loop may play a role in structural rearrangements at the translocation pore of glutamate transporter on account of its substrate-induced conformational shift of between TM4b-4c loop and TM7, HP1, or HP2. We also speculate that the TM4b-4c loop may take part in the transport pathway during the transport cycle.

Conflict of interests

Downloaded from molpharm.aspetjournals.org at ASPET Journals on April 17, 2024

Molecular Pharmacology Fast Forward. Published on October 22, 2018 as DOI: 10.1124/mol.118.113183
This article has not been copyedited and formatted. The final version may differ from this version.

The authors declare that there are no conflicts of interest regarding the publication of this paper.

Author Contributions:

Participated in research design: Qu.

Conducted Experiments: W.L. Zhang, X.P. Zhang.

Performed data analysis: W.L. Zhang, X.P. Zhang, Qu.

Wrote or contributed to the writing of the manuscript: W.L. Zhang, Qu.

Downloaded from molpharm.aspetjournals.org at ASPET Journals on April 17, 2024

Molecular Pharmacology Fast Forward. Published on October 22, 2018 as DOI: 10.1124/mol.118.113183
This article has not been copyedited and formatted. The final version may differ from this version.

References:

Akyuz N, Altman RB, Blanchard SC and Boudker O (2013) Transport dynamics in a glutamate transporter homologue. *Nature* **502**(7469): 114-118.

Amara SG and Fontana AC (2002) Excitatory amino acid transporters: keeping up with glutamate. *Neurochemistry international* **41**(5): 313-318.

Arriza JL, Eliasof S, Kavanaugh MP and Amara SG (1997) Excitatory amino acid transporter 5, a retinal glutamate transporter coupled to a chloride conductance. *Proceedings of the National Academy of Sciences of the United States of America* **94**(8): 4155-4160.

Arriza JL, Fairman WA, Wadiche JI, Murdoch GH, Kavanaugh MP and Amara SG (1994) Functional comparisons of three glutamate transporter subtypes cloned from human motor cortex. *The Journal of neuroscience : the official journal of the Society for Neuroscience* **14**(9): 5559-5569.

Bergles DE, Tzingounis AV and Jahr CE (2002) Comparison of coupled and uncoupled currents during glutamate uptake by GLT-1 transporters. *The Journal of neuroscience : the official journal of the Society for Neuroscience* **22**(23): 10153-10162.

Boudker O, Ryan RM, Yernool D, Shimamoto K and Gouaux E (2007) Coupling substrate and ion binding to extracellular gate of a sodium-dependent aspartate transporter. *Nature* **445**(7126): 387-393.

Brew H and Attwell D (1987) Electrogenic glutamate uptake is a major current carrier in the membrane of axolotl retinal glial cells. *Nature* **327**(6124): 707-709.

Canul-Tec JC, Assal R, Cirri E, Legrand P, Brier S, Chamot-Rooke J and Reyes N (2017) Structure and allosteric inhibition of excitatory amino acid transporter 1. *Nature* **544**(7651): 446-451.

Crisman TJ, Qu S, Kanner BI and Forrest LR (2009) Inward-facing conformation of glutamate transporters as revealed by their inverted-topology structural repeats. *Proceedings of the National Academy of Sciences of the United States of America* **106**(49): 20752-20757.

Fairman WA, Vandenberg RJ, Arriza JL, Kavanaugh MP and Amara SG (1995) An excitatory amino-acid transporter with properties of a ligand-gated chloride channel. *Nature* **375**(6532): 599-603.

Fuerst TR, Niles EG, Studier FW and Moss B (1986) Eukaryotic transient-expression system based on recombinant vaccinia virus that synthesizes bacteriophage T7 RNA polymerase. *Proceedings of the National Academy of Sciences of the United States of America* **83**(21): 8122-8126.

Glusker JP (1991) Structural aspects of metal liganding to functional groups in proteins. *Advances in protein chemistry* **42**: 1-76.

Grewer C, Balani P, Weidenfeller C, Bartusel T, Tao Z and Rauen T (2005) Individual subunits of the glutamate transporter EAAC1 homotrimer function independently of each other. *Biochemistry-Us* **44**(35): 11913-11923.

Groeneveld M and Slotboom DJ (2007) Rigidity of the subunit interfaces of the trimeric glutamate transporter GltT during translocation. *Journal of molecular biology* **372**(3): 565-570.

Grunewald M, Bendahan A and Kanner BI (1998) Biotinylation of Single Cysteine Mutants of the Glutamate Transporter GLT-1 from Rat Brain Reveals Its Unusual Topology. *Neuron* **21**(3): 623-632.

Downloaded from molpharm.aspetjournals.org at ASPET Journals on April 17, 2024

Molecular Pharmacology Fast Forward. Published on October 22, 2018 as DOI: 10.1124/mol.118.113183
This article has not been copyedited and formatted. The final version may differ from this version.

Grunewald M and Kanner B (1995) Conformational changes monitored on the glutamate transporter GLT-1 indicate the existence of two neurotransmitter-bound states. *The Journal of biological chemistry* **270**(28): 17017-17024.

Holmgren M, Liu Y, Xu Y and Yellen G (1996) On the use of thiol-modifying agents to determine channel topology. *Neuropharmacology* **35**(7): 797-804.

Kanai Y and Hediger MA (1992) Primary structure and functional characterization of a high-affinity glutamate transporter. *Nature* **360**(6403): 467-471.

Kanai Y and Hediger MA (2004) The glutamate/neutral amino acid transporter family SLC1: molecular, physiological and pharmacological aspects. *Pflugers Archiv : European journal of physiology* **447**(5): 469-479.

Kanner BI and Sharon I (1978) Active transport of L-glutamate by membrane vesicles isolated from rat brain. *Biochemistry-Us* **17**(19): 3949-3953.

Koch HP, Brown RL and Larsson HP (2007a) The glutamate-activated anion conductance in excitatory amino acid transporters is gated independently by the individual subunits. *The Journal of neuroscience : the official journal of the Society for Neuroscience* **27**(11): 2943-2947.

Koch HP, Hubbard JM and Larsson HP (2007b) Voltage-independent sodium-binding events reported by the 4B-4C loop in the human glutamate transporter excitatory amino acid transporter 3. *The Journal of biological chemistry* **282**(34): 24547-24553.

Koch HP and Larsson HP (2005) Small-scale molecular motions accomplish glutamate uptake in human glutamate transporters. *The Journal of neuroscience : the official journal of the Society for Neuroscience* **25**(7): 1730-1736.

Leary GP, Stone EF, Holley DC and Kavanaugh MP (2007) The glutamate and chloride permeation pathways are colocalized in individual neuronal glutamate transporter subunits. *The Journal of neuroscience : the official journal of the Society for Neuroscience* **27**(11): 2938-2942.

Lehre KP and Danbolt NC (1998) The number of glutamate transporter subtype molecules at glutamatergic synapses: chemical and stereological quantification in young adult rat brain. *The Journal of neuroscience : the official journal of the Society for Neuroscience* **18**(21): 8751-8757.

Leighton BH, Seal RP, Watts SD, Skyba MO and Amara SG (2006) Structural rearrangements at the translocation pore of the human glutamate transporter, EAAT1. *The Journal of biological chemistry* **281**(40): 29788-29796.

Levy LM, Warr O and Attwell D (1998) Stoichiometry of the glial glutamate transporter GLT-1 expressed inducibly in a Chinese hamster ovary cell line selected for low endogenous Na+-dependent glutamate uptake. *The Journal of neuroscience : the official journal of the Society for Neuroscience* **18**(23): 9620-9628.

Perez-Garcia MT, Chiamvimonvat N, Marban E and Tomaselli GF (1996) Structure of the sodium channel pore revealed by serial cysteine mutagenesis. *Proceedings of the National Academy of Sciences of the United States of America* **93**(1): 300-304.

Pines G, Danbolt NC, Bjoras M, Zhang Y, Bendahan A, Eide L, Koepsell H, Storm-Mathisen J, Seeberg E and Kanner BI (1992) Cloning and expression of a rat brain L-glutamate transporter. *Nature* **360**(6403): 464-467.

Pines G, Zhang Y and Kanner BI (1995) Glutamate 404 is involved in the substrate discrimination of GLT-1, a (Na+ + K+)-coupled glutamate transporter from rat brain. *The Journal of biological chemistry* **270**(29): 17093-17097.

Qu S and Kanner BI (2008) Substrates and non-transportable analogues induce structural rearrangements at the extracellular entrance of the glial glutamate

Downloaded from molpharm.aspetjournals.org at ASPET Journals on April 17, 2024

Molecular Pharmacology Fast Forward. Published on October 22, 2018 as DOI: 10.1124/mol.118.113183
This article has not been copyedited and formatted. The final version may differ from this version.

transporter GLT-1/EAAT2. *The Journal of biological chemistry* **283**(39): 26391-26400.

Reyes N, Ginter C and Boudker O (2009) Transport mechanism of a bacterial homologue of glutamate transporters. *Nature* **462**(7275): 880-885.

Rong X, Tan F, Wu X, Zhang X, Lu L, Zou X and Qu S (2016) TM4 of the glutamate transporter GLT-1 experiences substrate-induced motion during the transport cycle. *Scientific reports* **6**: 34522.

Rong X, Zomot E, Zhang X and Qu S (2014) Investigating substrate-induced motion between the scaffold and transport domains in the glutamate transporter EAAT1. *Molecular pharmacology* **86**(6): 657-664.

Seal RP and Amara SG (1998) A reentrant loop domain in the glutamate carrier EAAT1 participates in substrate binding and translocation. *Neuron* **21**(6): 1487-1498.

Seal RP, Leighton BH and Amara SG (2000) A model for the topology of excitatory amino acid transporters determined by the extracellular accessibility of substituted cysteines. *Neuron* **25**(3): 695-706.

Shlaifer I and Kanner BI (2007) Conformationally sensitive reactivity to permeant sulfhydryl reagents of cysteine residues engineered into helical hairpin 1 of the glutamate transporter GLT-1. *Molecular pharmacology* **71**(5): 1341-1348.

Shrivastava IH, Jiang J, Amara SG and Bahar I (2008) Time-resolved mechanism of extracellular gate opening and substrate binding in a glutamate transporter. *The Journal of biological chemistry* **283**(42): 28680-28690.

Slotboom DJ, Sobczak I, Konings WN and Lolkema JS (1999) A conserved serine-rich stretch in the glutamate transporter family forms a substrate-sensitive reentrant loop. *Proceedings of the National Academy of Sciences of the United States of America* **96**(25): 14282-14287.

Storck T, Schulte S, Hofmann K and Stoffel W (1992) Structure, expression, and functional analysis of a Na(+)-dependent glutamate/aspartate transporter from rat brain. *Proceedings of the National Academy of Sciences of the United States of America* **89**(22): 10955-10959.

Teichman S, Qu S and Kanner BI (2009) The equivalent of a thallium binding residue from an archeal homolog controls cation interactions in brain glutamate transporters. *Proceedings of the National Academy of Sciences of the United States of America* **106**(34): 14297-14302.

Verdon G and Boudker O (2012) Crystal structure of an asymmetric trimer of a bacterial glutamate transporter homolog. *Nature structural & molecular biology* **19**(3): 355-357.

Wadiche JI, Arriza JL, Amara SG and Kavanaugh MP (1995) Kinetics of a human glutamate transporter. *Neuron* **14**(5): 1019-1027.

Yernool D, Boudker O, Jin Y and Gouaux E (2004) Structure of a glutamate transporter homologue from Pyrococcus horikoshii. *Nature* **431**(7010): 811-818.

Zerangue N and Kavanaugh MP (1996) Flux coupling in a neuronal glutamate transporter. *Nature* **383**(6601): 634-637.

Zhang W, Zhang X and Qu S (2018) Cysteine Scanning Mutagenesis of TM4b-4c Loop of Glutamate Transporter EAAT1 Reveals Three Conformationally Sensitive Residues. *Molecular pharmacology*.

Downloaded from molpharm.aspetjournals.org at ASPET Journals on April 17, 2024

Molecular Pharmacology Fast Forward. Published on October 22, 2018 as DOI: 10.1124/mol.118.113183
This article has not been copyedited and formatted. The final version may differ from this version.

Footnotes:

This work was supported by the National Natural Science Foundation of China [Grant Nos. 31570716 and U1603281] and the Program for Changjiang Scholars and Innovative Research Team in University [IRT_16R37]

Downloaded from molpharm.aspetjournals.org at ASPET Journals on April 17, 2024

Molecular Pharmacology Fast Forward. Published on October 22, 2018 as DOI: 10.1124/mol.118.113183
This article has not been copyedited and formatted. The final version may differ from this version.

Figure Legends:

Fig. 1. Sequence alignment and EAAT transmembrane topology

(A), (B) Sequence alignment of TM4b-4c loop and TM7 on Glt_{Ph} and EAAT1 (Canul-Tec et al., 2017; Yernool et al., 2004). Insertions in eukaryotic transporters between helices 4b and 4c are not included and are marked by "------". Arrows represent residues V151, T308 and A326 of Glt_{Ph} which are equivalent to A243, T396, and A414 of EAAT1, respectively; (C) Representation of EAAT transmembrane topology (Yernool et al., 2004). The red dots show the approximate locations of the following cysteine substitutions: A243, T396 and A414.

Fig. 2. Inhibition of transport of cysteine mutants by CuPh.

(A) Effect of CuPh on the transport activity of cysteine mutants; (B), (C) Effect of different concentrations of CuPh on the transport activity of A243C/T396C, A243C/A414C and CL-EAAT1; (D) Effect of 600 μM CuPh on D-[^{3}H]-aspartate uptake HeLa cells expressing CL-EAAT1, single cysteine mutants (A243C, T396C and A414C), double cysteine mutants (A243C/T396C and A243C/A414C), or cells co-transfected with single-cystein mutants (A243C co T396C or A243C co A414C). (A-D) Cells expressing mutants and CL-EAAT1 were treated with CuPh in NaCl solution for 5 min at room temperature, and subsequently D-[^{3}H]-aspartate transport was assayed. Data represent percentage of the remaining uptake activity after incubation with CuPh relative to the values obtained in the absence of CuPh and represent as mean ± S.D. of four different experiments done in triplicate, $^{**}P < 0.01$ versus CL-EAAT1 using one-way analysis of variance (n = 4). (E) Transport activity of cysteine mutants and CL-EAAT1. Data are given as a percentage of cysteine-less EAAT1 transport activity and shown as the mean ± SD of three experiments. Values that are statistically significant different from those of CL-EAAT1 were determined by one-way ANOVA ($^{*}P < 0.05$; $^{**}P < 0.01$, n = 3).

Fig. 3. D-[^{3}H]-Asp uptake activity and membrane expression of mutants.

HeLa cells were transfected with CL-EAAT1 and other constructed mutants. (A) The total proteins, biotinylated membrane proteins and non-biotinylated proteins were measured by western blot as described under Materials and Methods. Blots of all proteins were probed with the anti-EAAT1 antibody. Each blot of the biotinylated membrane proteins was probed for the internal plasma membrane marker-integrin and the absence of α/β-tubulin (an endogenous cytosolic protein representing the negative control) in the biotinylated membrane proteins. Each blot of the non-biotinylated proteins was probed for the presence of α/β-tubulin. Each blot of the total proteins was probed for the presence of actin. (B) Densitometric analysis of the total proteins for each mutant is normalized to the internal marker (β-actin) and

Downloaded from molpharm.aspetjournals.org at ASPET Journals on April 17, 2024

Molecular Pharmacology Fast Forward. Published on October 22, 2018 as DOI: 10.1124/mol.118.113183
This article has not been copyedited and formatted. The final version may differ from this version.

represented as a percentage of CL-EAAT1. (C) Densitometric analysis of the biotinylated membrane proteins for each mutant is normalized to the internal marker (integrin) and represented as a percentage of CL-EAAT1. (D) Densitometric analysis of the non-biotinylated proteins for each mutant is normalized to the internal marker (α/β-tubulin) and represented as a percentage of CL-EAAT1. (E) D-[^{3}H]-Asp uptake activity is normalized to relative cell surface expression. (F) The ratio of the biotinylated membrane protein expression and non-biotinylated protein expression of CL-EAAT1 and mutants. Values represent as the mean ± SD of three different experiments done in triplicates. Values that are statistically significant different from that of CL-EAAT1 were determined by one-way ANOVA (*P < 0.05, n = 3; **P < 0.01, n = 3).

Fig. 4. The effect of DTT on the CuPh mediated inhibition and inhibition of cadmium on mutants.

HeLa cells expressing A243C/T396C (A) or A243C/A414C (B) were pre-incubated for 5 min in the presence or absence of 600 μM CuPh and then incubated with or without 20 mM DTT. D-[^{3}H]-Asp uptake was measured. Values are shown as a percentage of the uptake in mutants without CuPh and DTT treatment and represent as the mean ± SD for four independent experiments. Values from incubation by CuPh(+), DTT(-) are statistically significant different from incubation by CuPh(-), DTT(-) or CuPh(+), DTT(+). (**P < 0.01, n = 4). HeLa cells expressing A243C/T396C (C), A243C/A414C (D) or the indicated control were washed once with choline chloride–containing solution and assayed for transport in the presence or absence of 500 μM cadmium chloride. Values shown are the percentage activity in the presence of 500 μM cadmium chloride relative to that in its absence. Values represent the mean ± SD of four different experiments done in triplicate. **P < 0.01 versus CL-EAAT1 using one-way analysis of variance (n = 4).

Fig. 5. Effect of external media on the inhibition of transport activity by CuPh

HeLa cells expressing A243C/T396C (A), A243C/A414C (B) were pre-incubated for 5 min in the presence or absence of 600 μM CuPh. The indicated pre-incubation solutions contained NaCl solution, NaCl solution +1 mM L-glutamate, NaCl solution +20 μM TBOA, KCl solution, ChCl solution. After washing, D-[^{3}H]-aspartate uptake was measured. Values are given as percentage of control (pre-incubation without CuPh) and represent mean ± SD for four different experiments done in triplicate. *P < 0.05; **P < 0.01 versus NaCl group using one-way analysis of variance (n = 4).

Downloaded from molpharm.aspetjournals.org at ASPET Journals on April 17, 2024

Molecular Pharmacology Fast Forward. Published on October 22, 2018 as DOI: 10.1124/mol.118.113183
This article has not been copyedited and formatted. The final version may differ from this version.

Fig. 6. Effect of external media on the inhibition of transport activity by MTSET or MTSEA in T396C and A414C

Dose-response effects of MTSET (A) or MTSEA (C) on D-[^{3}H]-Asp transport activity of CL-EAAT1, T396C and A414C; (B) HeLa cells expressing A414C were pre-incubated in the presence or absence of 1.0 mM MTSET for 5 min in different external media that contained NaCl solution, NaCl solution +1 mM L-glutamate, NaCl solution +20 μM TBOA, KCl solution, or ChCl solution. HeLa cells expressing T396C (D) and A414C (E) were pre-incubated in the presence or absence of 3.0 (D), 2.5 (E) mM MTSEA for 5 min in different external media that contained NaCl solution, NaCl solution +1 mM L-glutamate, NaCl solution +20 μM TBOA, KCl solution, or ChCl solution. D-[^{3}H]-aspartate uptake was measured. Values are given as percentage of control (pre-incubation without MTSET or MTSEA) and represent mean ± SD of four different experiments done in triplicate. $^{**}P < 0.01$ versus NaCl group using one-way analysis of variance (n = 4).

Fig. 7. The substrate-binding, outward-facing, and inward-facing structures of Glt_{Ph}.

The crystallized substrate binding (A), outward-facing (B), and inward-facing (C) forms of Glt_{Ph} are shown (respective PDB ID codes 1XFH, 2NWW, and 3KBC), aligned using TM1 (blue), TM2 (purple), TM 4 (light green), TM 5 (green), and TM 7 (light orange). Cα-atoms of the indicated residues V151(red), T308 (light orange), and A326 (light orange) are equivalent to A243, T396, and A414 of CL-EAAT1, respectively. Proximity is showed by discontinuous black lines.

Downloaded from molpharm.aspetjournals.org at ASPET Journals on April 17, 2024

Molecular Pharmacology Fast Forward. Published on October 22, 2018 as DOI: 10.1124/mol.118.113183
This article has not been copyedited and formatted. The final version may differ from this version.

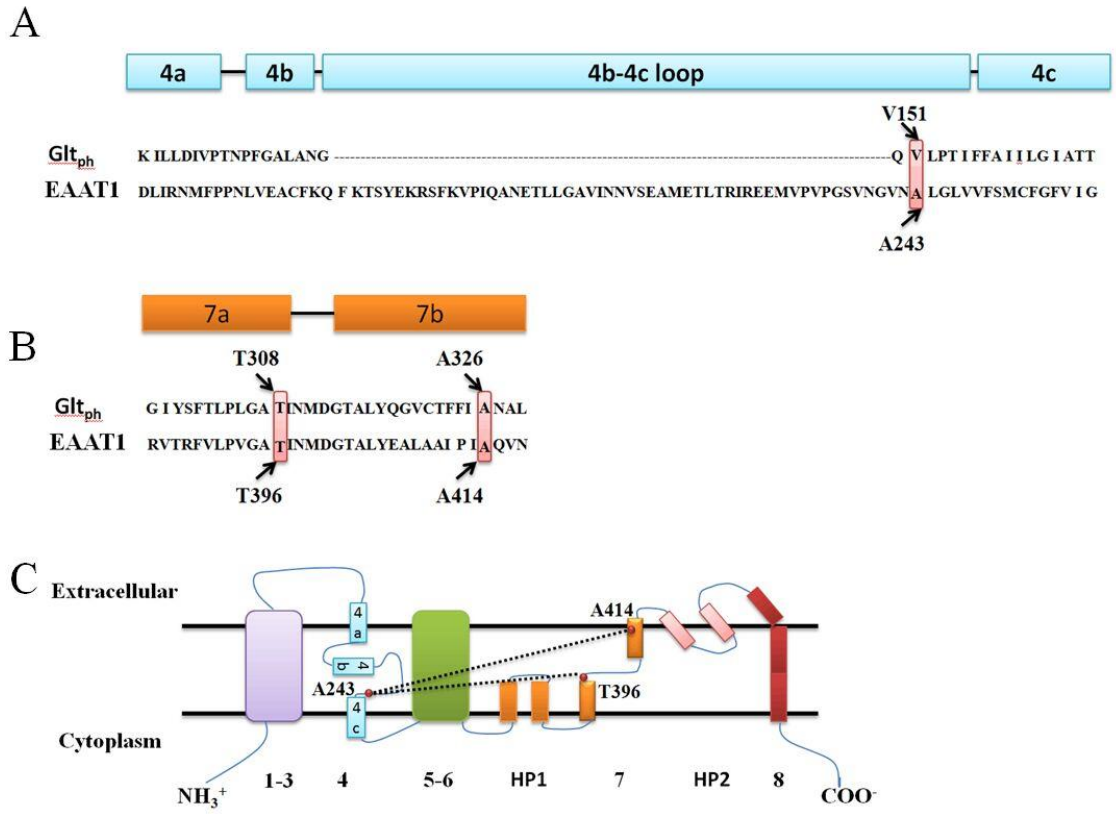

Fig. 1.

Downloaded from molpharm.aspetjournals.org at ASPET Journals on April 17, 2024

Molecular Pharmacology Fast Forward. Published on October 22, 2018 as DOI: 10.1124/mol.118.113183
This article has not been copyedited and formatted. The final version may differ from this version.

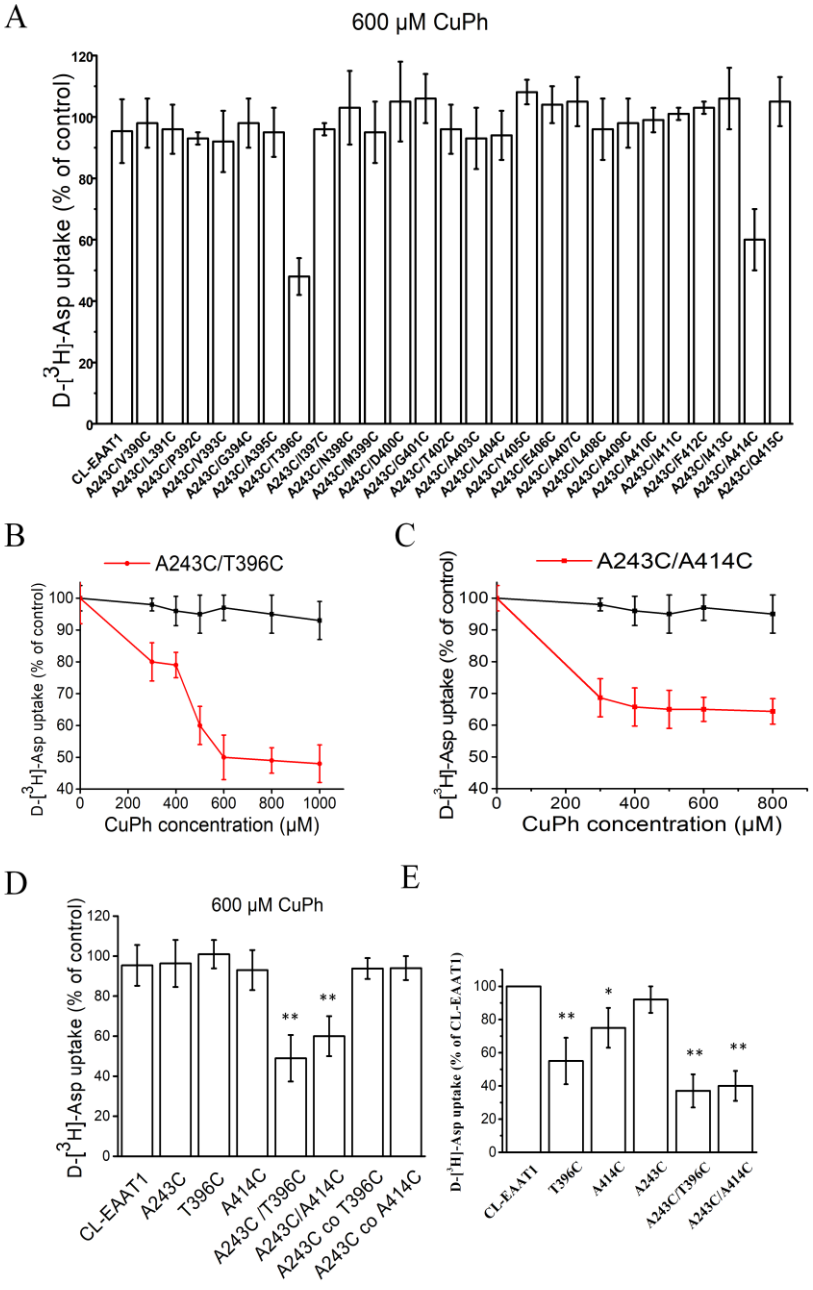

Fig. 2.

Downloaded from molpharm.aspetjournals.org at ASPET Journals on April 17, 2024

Molecular Pharmacology Fast Forward. Published on October 22, 2018 as DOI: 10.1124/mol.118.113183
This article has not been copyedited and formatted. The final version may differ from this version.

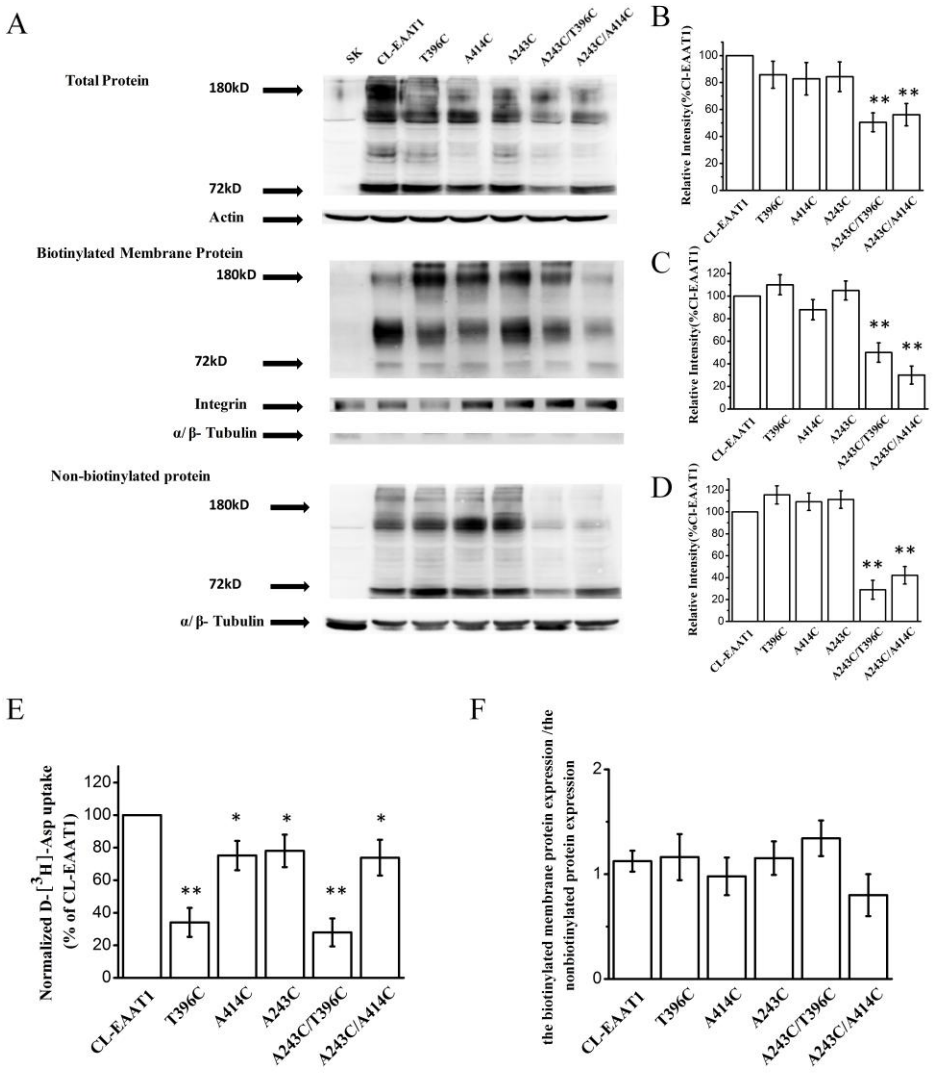

Fig. 3.

Downloaded from molpharm.aspetjournals.org at ASPET Journals on April 17, 2024

Molecular Pharmacology Fast Forward. Published on October 22, 2018 as DOI: 10.1124/mol.118.113183
This article has not been copyedited and formatted. The final version may differ from this version.

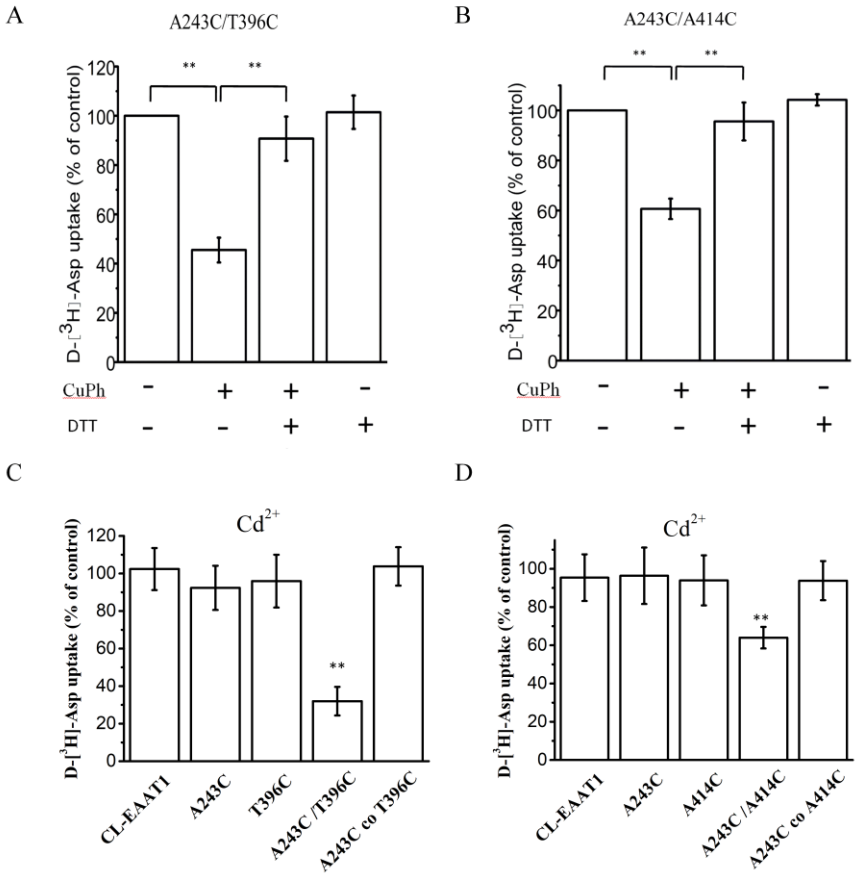

Fig. 4.

Downloaded from molpharm.aspetjournals.org at ASPET Journals on April 17, 2024

Molecular Pharmacology Fast Forward. Published on October 22, 2018 as DOI: 10.1124/mol.118.113183
This article has not been copyedited and formatted. The final version may differ from this version.

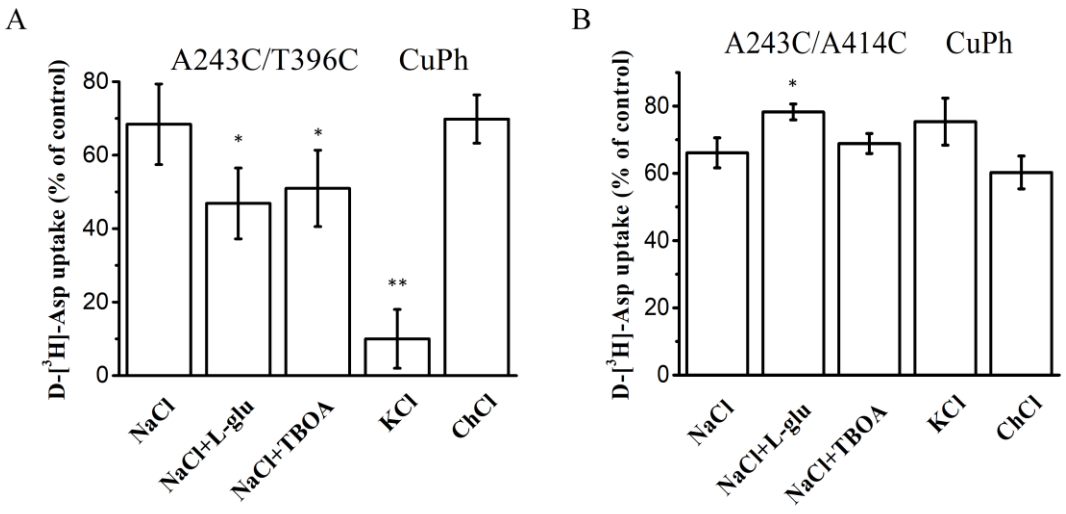

Fig. 5.

Downloaded from molpharm.aspetjournals.org at ASPET Journals on April 17, 2024

Molecular Pharmacology Fast Forward. Published on October 22, 2018 as DOI: 10.1124/mol.118.113183
This article has not been copyedited and formatted. The final version may differ from this version.

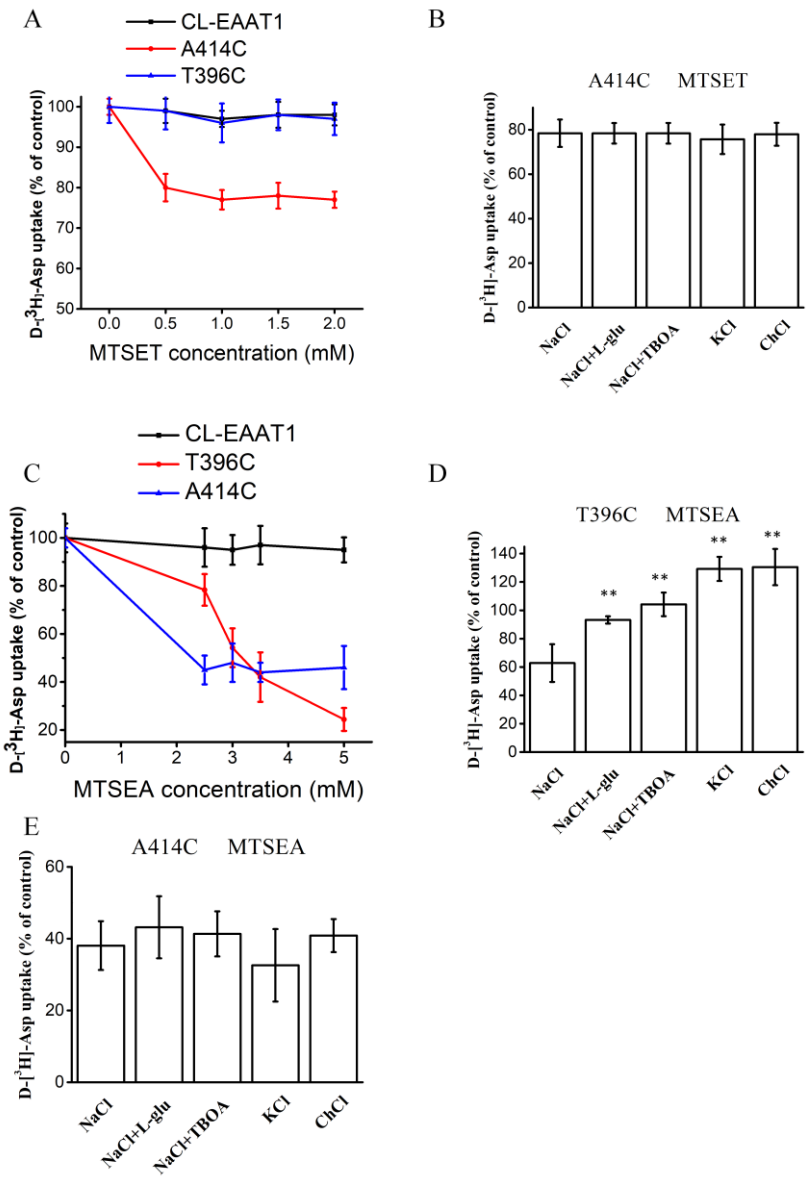

Fig. 6.

Downloaded from molpharm.aspetjournals.org at ASPET Journals on April 17, 2024

Molecular Pharmacology Fast Forward. Published on October 22, 2018 as DOI: 10.1124/mol.118.113183
This article has not been copyedited and formatted. The final version may differ from this version.

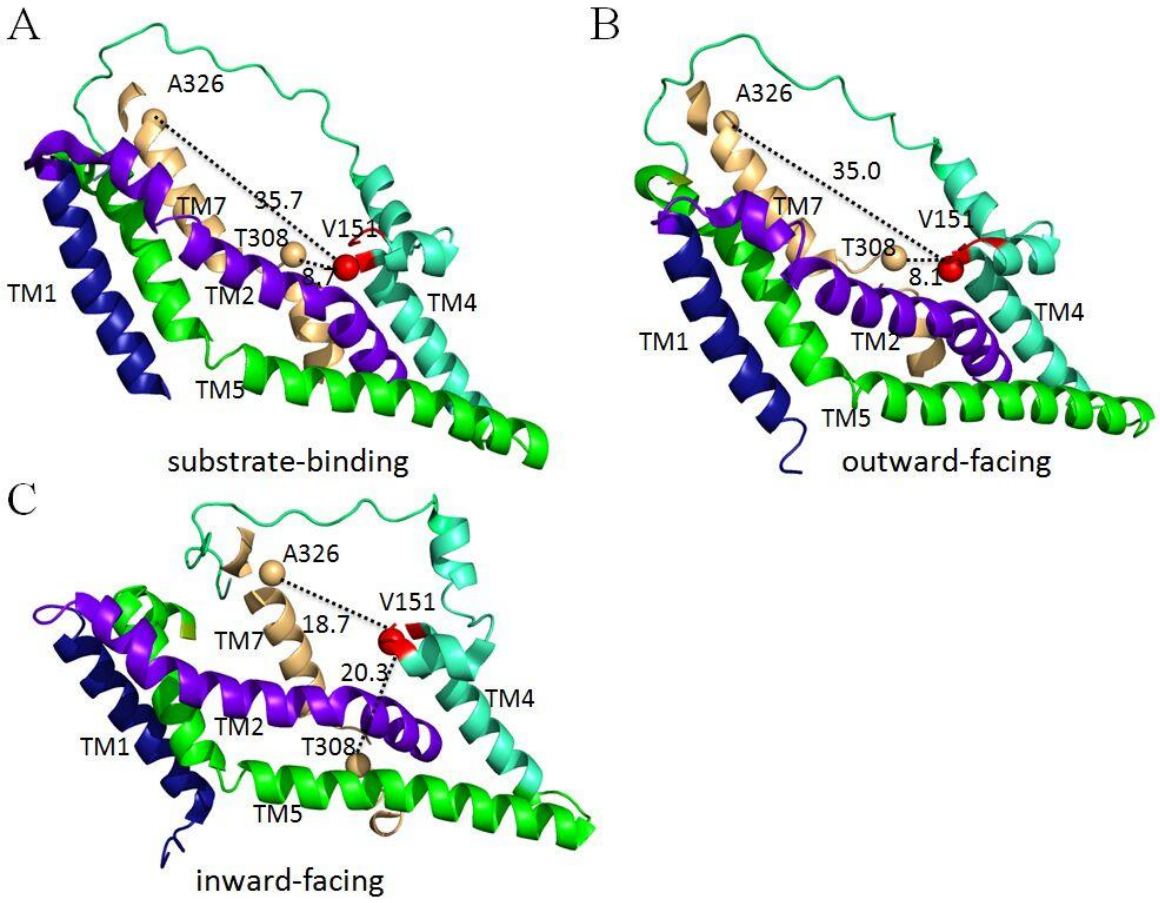

Fig. 7.

Downloaded from molpharm.aspetjournals.org at ASPET Journals on April 17, 2024